Supporting Material

# An Integrated Mitochondrial ROS Production and Scavenging Model: Implications for Heart Failure

Laura D. Gauthier[‡], Joseph L. Greenstein[‡],

Brian O'Rourke[†], and Raimond L. Winslow[‡],

[†]Division of Cardiology, Johns Hopkins University School of Medicine, Baltimore, Maryland, USA and [‡]Institute for Computational Medicine, Baltimore, Maryland, USA

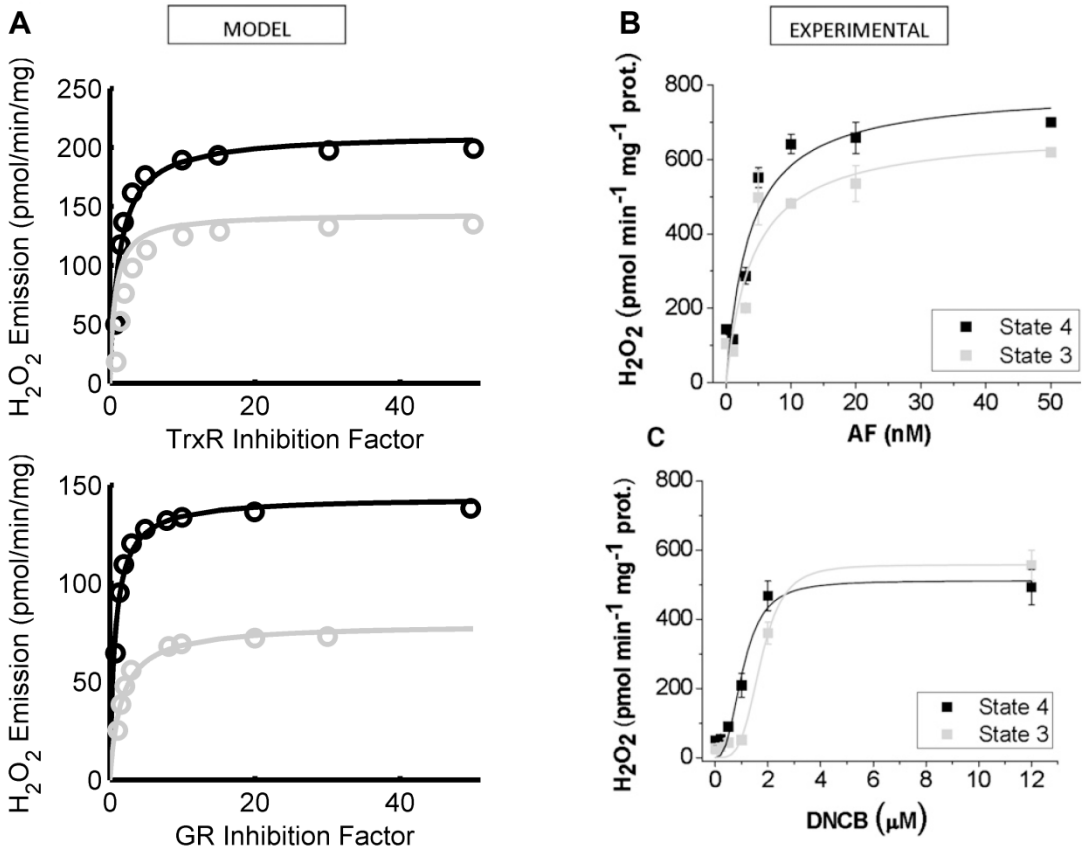


**Figure S1 Steady-state mitochondrial $H_2O_2$ emission during inhibitory titration of GR and TrxR in state 3 and state 4.** The model shows higher mitochondrial $H_2O_2$ emission in state 4 (black) than state 3 (blue) for both GR inhibition (A) and TrxR inhibition (B). As in the experimental data of Aon et al. (1), maximal $H_2O_2$ emission is greater under TrxR inhibition than under inhibition of GR.

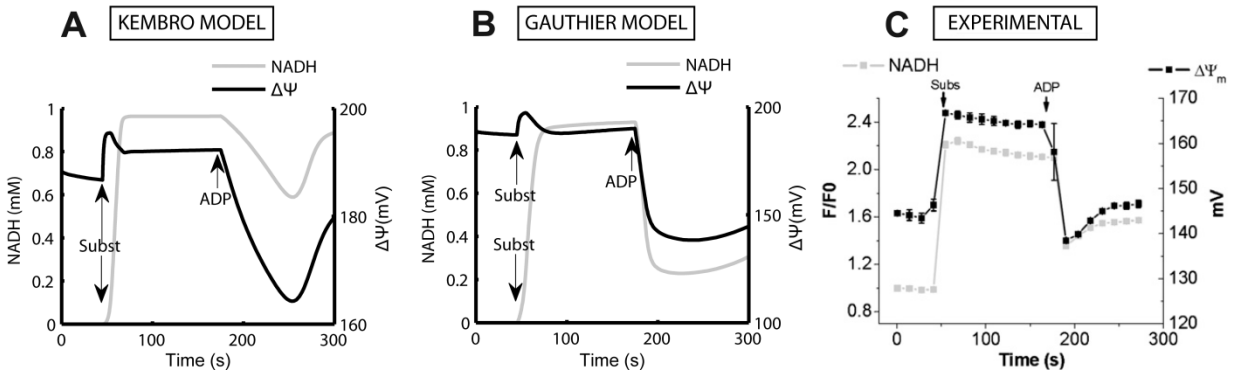


**Figure S2 NADH and ΔΨ dynamics for state 0 to state 4 to state 3 transitions. (A)**Kembro et al. model substrate addition (indicated by "Subst") was simulated as an increase in AcCoA and glutamate from $1x10^{-5}$ to 0.1 and $1x10^{-5}$ to 30, respectively. ADP addition represents an increase in extra-matrix ADP concentration from 0.01mM to 0.03mM, as in Kembro et al. (2), to simulate the state 4 to state 3 transition. **(B)**The same protocol for the model presented here. **(C)**Experimental data from Kembro et al. (2) show the results of the addition of 5mM G/M ("Subst") followed by 1mM ADP.

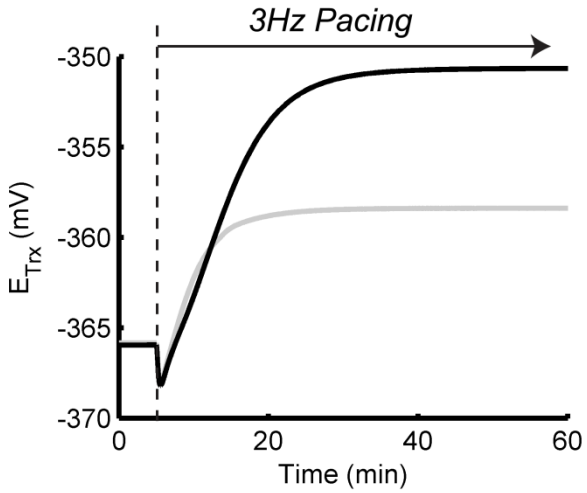


**Figure S3 Thioredoxin redox potential under mCU inhibition.** Decreases in NADPH also drive the oxidation of mitochondrial $Trx(SH)_2$ under control conditions (gray) and more extensively in the presence of mCU inhibition (black).

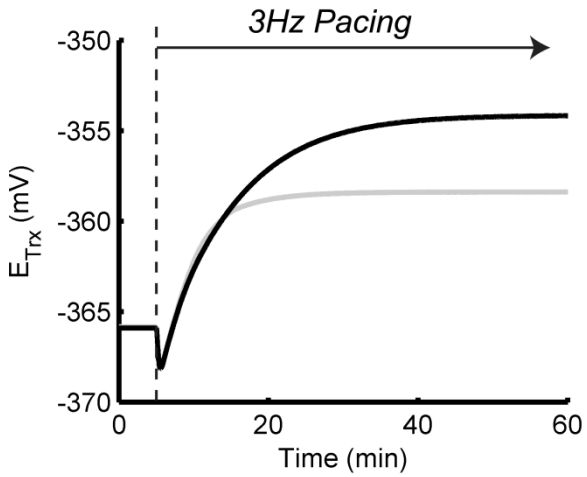


**Figure S4 Elevated $[Na^+]_i$ depletes thioredoxin pool.** 15mM $[Na^+]_i$ conditions (black) lead to a larger oxidation of the mitochondrial thioredoxin pool after the onset of pacing compared with control conditions (gray).

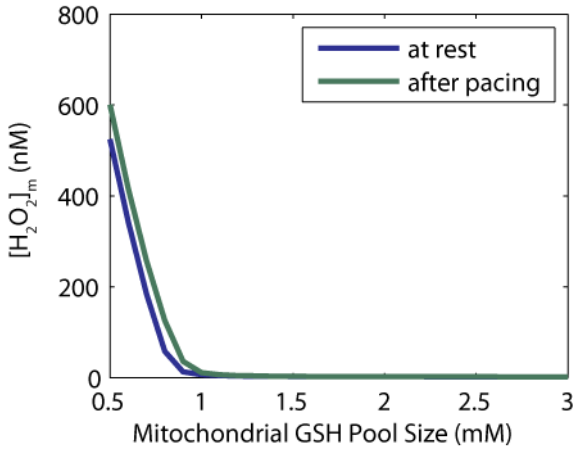


**Figure S5: Decreased mitochondrial GSH pool size elevates resting $[H_2O_2]_m$.** As the mitochondrial GSH pool size is decreased from 3mM to 1mM, resting $[H_2O_2]_m$ increases slightly. For decreases beyond 1mM, resting $[H_2O_2]_m$ is significantly elevated.

Notes on table 1:

Respiratory flux is given as (VNO+$VO_2$SDH) for Kembro et al. model (in units of mM O/ms) or 2*VO2 (where VO2 is actually in units of mM $O_2$/ms) for this model, then adjusted to match the experimental data units with a scale factor of 2*60e3 to convert from mM/ms to nmol/min/mg protein.

# Mitochondrial ROS Production and Scavenging Model

**Table S1 System of differential and algebraic equations used in the ME-R model**

| | |
|---|---|
| $\frac{d[Ca^{2+}]_m}{dt} = \delta_{Ca}\left(V_{uni} - V_{NaCa}\right)$ | (S4) |
| $\frac{d\,[ADP]_m}{dt} = V_{ANT} - V_{ATPase} - V_{SL}$ | (S5) |
| $\frac{d\Delta\Psi_m}{dt} = \frac{V_{He} + V_{He(SDH)} - V_{Hu} - V_{ANT} - V_{Hleak} - V_{NaCa} - 2V_{uni} - V_{IMAC}}{C_{mito}}$ | (S6) |
| $\frac{d[NADH]_m}{dt} = V_{O_2} + V_{IDH} + V_{KGDH} + V_{MDH} - V_{THD}$ | (S7) |
| $\frac{d[H^+]_m}{dt} = \delta_M\left(-V_{He} - V_{He(SDH)} + V_{Hu} + V_{NaH} + V_{PiC} + V_{Hleak}\right)$ | (S8) |
| $\frac{d[Pi]_m}{dt} = -V_{ATPase} + V_{PiC} - V_{SL}$ | (S9) |
| $\frac{d[ISOC]}{dt} = V_{ACO} - V_{IDH} - V_{IDH\_NADP}$ | (S10) |
| $\frac{d[\alpha KG]}{dt} = V_{IDH} + V_{IDH\_NADP} - V_{KGDH} + V_{ATT}$ | (S11) |
| $\frac{d[SCoA]}{dt} = V_{KGDH} - V_{SL}$ | (S12) |
| $\frac{d[Suc]}{dt} = V_{SL} - V_{O_2SDH}$ | (S13) |
| $\frac{d[FUM]}{dt} = V_{O_2SDH} - V_{FH}$ | (S14) |
| $\frac{d[MAL]}{dt} = V_{FH} - V_{MDH}$ | (S15) |
| $\frac{d[OAA]}{dt} = V_{MDH} - V_{CS} - V_{AAT}$ | (S16) |
| $\frac{d[NADPH]_m}{dt} = V_{IDH\_NADP} + V_{THD} - V_{GRm} - V_{TxRm}$ | (S17) |
| $\frac{d[O_2^{\cdot-}]_m}{dt} = shunt\left(V_{O_2} + V_{O_2SDH}\right) - V_{MnSOD} - V_{ROS}^{Tr}$ | (S18) |
| $\frac{d[O_2^{\cdot-}]_i}{dt} = \frac{v_m}{v_i}V_{ROS}^{Tr} - V_{CuZnSOD}$ | (S19) |
| $\frac{d[H_2O_2]_m}{dt} = \frac{1}{2}V_{MnSOD} - V_{difH_2O_2} - V_{GPXm} - V_{TxPXm}$ | (S20) |

$$\frac{d[H_2O_2]_i}{dt} = \frac{1}{2}V_{CuZnSOD} + \frac{v_m}{v_i}V_{difH_2O_2} - V_{GPXi} - V_{TxPXi} - V_{CAT} \quad \text{(S21)}$$

$$\frac{d[GSH]_m}{dt} = V_{GRm} - V_{GPXm} - V_{GRXm} + V_{GST} - V_{PSSGm} \quad \text{(S22)}$$

$$\frac{d[GSH]_i}{dt} = V_{GRi} - V_{GPXi} - V_{GRXi} + \frac{v_m}{v_i}V_{GST} - V_{PSSGi} \quad \text{(S23)}$$

$$\frac{d[GSSG]_m}{dt} = 0.5(V_{GPXm} - V_{GRm}) + V_{GRXm} \quad \text{(S24)}$$

$$\frac{d[TxR]_m}{dt} = V_{TxRm} - V_{TxPXm} \quad \text{(S25)}$$

$$\frac{d[TxR]_i}{dt} = V_{TxRi} - V_{TxPXi} \quad \text{(S26)}$$

$$\frac{d[PSSG]_m}{dt} = V_{PSSGm} - V_{GRXm} \quad \text{(S27)}$$

$$\frac{d[PSSG]_i}{dt} = V_{PSSGi} - V_{GRXi} \quad \text{(S28)}$$

Note that the differential equations for H2O2 contain corrections with regard to the stoichiometry of superoxide dismutase flux.

## Computational modeling of Reactive Oxygen Species scavenging systems

The upgraded two-compartment computational model of mitochondrial energetics-redox (ME-R) includes: (i) a complete array of antioxidant defenses in two compartments: mitochondrial matrix and extra-matrix (e.g. intermembrane space, cytoplasm); and (ii) two of the three main NADPH providers in mitochondria: $NADP^+$-dependent isocitrate dehydrogenase (IDH2) in the TCA cycle, and transhydrogenase (THD). In this section we will provide a detailed description of the antioxidant defenses and mitochondrial NADPH handling.

### Modeling superoxide dismutase

$$V_{MnSOD} = \frac{2\,k^1_{SOD}\,k^5_{SOD}\left(k^1_{SOD} + k^3_{SOD}\left(1 + \frac{[H_2O_2]_m}{K_i^{H_2O_2}}\right)\right)E^T_{MnSOD}\,[O_2^{\cdot-}]_m}{k^5_{SOD}\left(2\,k^1_{SOD} + k^3_{SOD}\left(1 + \frac{[H_2O_2]_m}{K_i^{H_2O_2}}\right)\right) + [O_2^{\cdot-}]_m\,k^1_{SOD}\,k^3_{SOD}\left(1 + \frac{[H_2O_2]_m}{K_i^{H_2O_2}}\right)} \quad \text{(S29)}$$

$$V_{CuZnSOD} = \frac{2\,k^1_{SOD}\,k^5_{SOD}\left(k^1_{SOD} + k^3_{SOD}\left(1 + \frac{[H_2O_2]_i}{K_i^{H_2O_2}}\right)\right)E^T_{CuZnSOD}\,[O_2^{\cdot-}]_i}{k^5_{SOD}\left(2\,k^1_{SOD} + k^3_{SOD}\left(1 + \frac{[H_2O_2]_i}{K_i^{H_2O_2}}\right)\right) + [O_2^{\cdot-}]_i\,k^1_{SOD}\,k^3_{SOD}\left(1 + \frac{[H_2O_2]_i}{K_i^{H_2O_2}}\right)} \quad \text{(S30)}$$

### $H_2O_2$ transport

$H_2O_2$ can diffuse freely between the two compartments, following the equation:

$$V_{diff_{H_2O_2}} = c_{diff_{H_2O_2}}([H_2O_2]_m - [H_2O_2]_i) \quad \text{(S31)}$$

## Gluthathione and glutaredoxin systems

The gluthathione system was present in both mitochondrial matrix and extra-matrix compartments and expressed as a system of equations comprising glutathione peroxidase ($V_{GPx}$) and reductase ($V_{GR}$) activities. The rate expressions for $V_{GPx}$ and $V_{GR}$ used in the model were formulated as described in our mitochondrial model of ROS metabolism (3).

$$V_{GPX_m} = \frac{E_T^{GPXm}[\mathrm{H_2O_2}]_\mathrm{m}\,[\mathrm{GSH}]_\mathrm{m}}{\Phi_1[\mathrm{GSH}]_\mathrm{m} + \Phi_2[\mathrm{H_2O_2}]_\mathrm{m}} \quad \text{(S32)}$$

$$V_{GPX_i} = \frac{E_T^{GPXi}[\mathrm{H_2O_2}]_\mathrm{i}\,[\mathrm{GSH}]_\mathrm{i}}{\Phi_1[\mathrm{GSH}]_\mathrm{i} + \Phi_2[\mathrm{H_2O_2}]_\mathrm{i}} \quad \text{(S33)}$$

$$V_{GR_m} = \frac{k_{GR}^1\ E_T^{GRm}}{1+\frac{K_M^{GSSG}}{[\mathrm{GSSG}]}+\frac{K_M^{NADPH}}{[\mathrm{NADPH}]_\mathrm{m}}+\frac{K_M^{GSSG}\ K_M^{NADPH}}{[GSSG]_m[\mathrm{NADPH}]_\mathrm{m}}} \quad \text{(S34)}$$

$$V_{GR_i} = \frac{k_{GR}^1\ E_T^{GRi}}{1+\frac{K_M^{GSSG}}{V_{GSS}}+\frac{K_M^{NADPH}}{[\mathrm{NADPH}]_\mathrm{i}}+\frac{K_M^{GSSG}\ K_M^{NADPH}}{[GSSG]_i[\mathrm{NADPH}]_\mathrm{i}}} \quad \text{(S35)}$$

The glutaredoxin system can then detoxify the glutathionylated proteins and uses GSH as cofactor (4, 5).

$$V_{GRX_m} = \frac{k_{grx_m}\ K_{eq}^{GRX}\ ([GSH]_m)^2\ GrxT\ [PSSG]_m}{([\mathrm{GSSG}]_\mathrm{m}+K_{eq}^{GRX}\ ([GSH]_m)^2)\left(\frac{K_{eq}^{GRX}\ ([GSH]_m)^2\ GrxT}{[\mathrm{GSSG}]_\mathrm{m}+K_{eq}^{GRX}\ ([GSH]_m)^2}+K_m^{Grx}\right)([\mathrm{PSSG}]_\mathrm{m}+K_m^{PSSG})} \quad \text{(S36)}$$

$$V_{GRX_i} = \frac{k_{grx_i}\ K_{eq}^{GRX}\ ([GSH]_i)^2\ GrxT\ [PSSG]_i}{(\mathrm{V_{GSS}}+K_{eq}^{GRX}\ ([GSH]_i)^2)\left(\frac{K_{eq}^{GRX}\ ([GSH]_i)^2\ GrxT}{[GSSG]_i+K_{eq}^{GRX}\ ([GSH]_i)^2}+K_m^{Grx}\right)([\mathrm{PSSG}]_\mathrm{i}+K_m^{PSSG})} \quad \text{(S37)}$$

$$V_{PSSG_m} = \frac{k_{PSH}^1\ E_T^{PSH}\ (PSSGT-[PSSG]_m)}{\left(1+\frac{K_M^{GSH}}{[GSH]_m}\right)\left(1+\frac{[H_2O_2]_m}{K_{act}^{H2O2}}\right)} \quad \text{(S38)}$$

$$V_{PSSG_i} = \frac{k_{PSH}^1\ E_T^{PSH}\ (PSSGT-[PSSG]_i)}{\left(1+\frac{K_M^{GSH}}{[GSH]_i}\right)\left(1+\frac{[H_2O_2]_i}{K_{act}^{H2O2}}\right)} \quad \text{(S39)}$$

We have assumed that the total pool of glutathione, $G_T$, is conserved, as indicated by equation S40, and from there the GSSG concentration in the extra-matrix compartment can be estimated (Eq. S41).

$$\mathrm{G}_T = \mathrm{G}_T - [\mathrm{GSH}]_\mathrm{m} - [\mathrm{GSH}]_i - 2\,[\mathrm{GSSG}] - [\mathrm{PSSG}]_\mathrm{m} - [\mathrm{PSSG}]_\mathrm{i} - 2\,[GSSG]_i \quad \text{(S40)}$$

$$[\mathrm{GSSG}]_i = 0.5\ (\mathrm{G}_T - [\mathrm{GSH}]_\mathrm{m} - [\mathrm{GSH}]_i - 2\ [\mathrm{GSSG}]_\mathrm{m} - [\mathrm{PSSG}]_\mathrm{m} - [\mathrm{PSSG}]_\mathrm{i}) \quad \text{(S41)}$$

In addition we have included passive GSH transport ($V_{GST}$) across the inner mitochondrial membrane.

$$V_{GST} = c_{GST}\frac{([GSH]_i - [GSH]_m)}{[GSH]_i + k_{0.5}^{GST}} \quad \text{(S42)}$$

**Thioredoxin system**

The Trx system includes peroxiredoxin ($V_{Prx3}$) and thioredoxin reductase ($V_{TrxR}$) (6). The rate expression for $V_{TPrx3}$ was derived on the basis of the experimental studies performed by (7), from which we also obtained the rate constants. $V_{TrxR}$ represents a Michaelis-Menten rate expression with two substrates (NADPH and Trx(SS) with kinetic parameters derived from refs. (8) and (9).

$$V_{Prx3_m} = \frac{E_T^{Prx3m}[H_2O_2]_m\ [TrxSH_2]_m}{\Phi_{1Prx}[TrxSH_2]_m + \Phi_{2Prx}[H_2O_2]_m} \quad \text{(S43)}$$

$$V_{Prx_i} = \frac{E_T^{Prxi}[\mathrm{H_2O_2}]_\mathrm{i}\ [\mathrm{TrxSH_2}]_\mathrm{i}}{\Phi_{1Prx}[\mathrm{TrxSH_2}]_\mathrm{i} + \Phi_{2Prx}[\mathrm{H_2O_2}]_i} \quad \text{(S44)}$$

$$V_{TrxR_m} = \frac{k_{TrxR}^1\ E_T^{TrxR2m}}{1 + \frac{K_M^{TrxSS}}{[TrxSS]_m} + \frac{K_{Mtrx}^{NADPH}}{[NADPH]_m} + \frac{K_M^{TrxSS}}{[TrxSS]_m}\frac{K_{Mtrx}^{NADPH}}{[NADPH]_m}} \quad \text{(S45)}$$

$$V_{TrxR_i} = \frac{k_{TrxR}^1\ E_T^{TrxRi}}{1 + \frac{K_M^{TrxSS}}{[TrxSS]_i} + \frac{K_{Mtrx}^{NADPH}}{[NADPH]_i} + \frac{K_M^{TrxSS}}{[TrxSS]_i}\frac{K_{Mtrx}^{NADPH}}{[NADPH]_i}} \quad \text{(S46)}$$

$$[\mathrm{TrxSS}]_\mathrm{m} = TrxT_m - [\mathrm{TrxSH_2}]_\mathrm{m} \quad \text{(S47)}$$

$$[\mathrm{TrxSS}]_\mathrm{i} = TrxT_i - [\mathrm{TrxSH_2}]_\mathrm{i} \quad \text{(S48)}$$

**Extra-matrix Catalase**

$$V_{CAT} = 2k_{CAT}^1 E_{CAT}^T [\mathrm{H_2O_2}]_\mathrm{i} e^{-fr[\mathrm{H_2O_2}]_\mathrm{i}}$$

Scavenging parameters are the same as in Kembro et al. with the exception of enzyme concentrations for GR and Trx, which were adjusted to match the proportional control of scavenging demonstrated in Figure 4.2.

**Table S2 Parameter values used in the simulations: ROS production and scavenging – mitochondrial model**

| Symbol | Value | Units | Description | Eq | Reference |
|---|---|---|---|---|---|
| $k_{SOD}^{1}$ | $1.2\times10^{3}$ | $mM^{-1}ms^{-1}$ | Second-order rate constant of SOD | S29,S30 | (2) |
| $k_{SOD}^{3}$ | 24 | $mM^{-1}ms^{-1}$ | Second-order rate constant of SOD | S29,S30 | (2) |
| $k_{SOD}^{5}$ | $2.4\times10^{-4}$ | $ms^{-1}$ | First-order rate constant of SOD | S29,S30 | (2) |
| $K_{i}^{H_2O_2}$ | 0.5 | mM | Inhibition constant for $H_2O_2$ | S29,S30 | (2) |
| $E_{MnSOD}^{T}$ | $3\times10^{-4}$ | mM | Mitochondrial matrix concentration of MnSOD | S29 | (2) |
| $E_{CuZnSOD}^{T}$ | $2.4\times10^{-4}$ | mM | Concentration of Cu,ZnSOD | S30 | (2) |
| $c_{diff_{H_2O_2}}$ | $2\times10^{-4}$ | $ms^{-1}$ | Diffusion constant for $H_2O_2$ | S31 | (2) |
| $\Phi_1$ | $5.0\times10^{-3}$ | mM ms | Constant for GPX activity | S32,S33 | (2) |
| $\Phi_2$ | 0.75 | mM ms | Constant for GPX activity | S32,S33 | (2) |
| $E_T^{GPXm}$ | $1\times10^{-4}$ | mM | Mitochondrial matrix concentration of GPX | S32 | (2) |
| $E_T^{GPXi}$ | $5\times10^{-5}$ | mM | Extra-matrix concentration of GPX | S33 | (2) |
| $k_{GR}^{1}$ | $2.5\times10^{-3}$ | $ms^{-1}$ | Catalytic constant of GR | S34,S35 | (2) |
| $E_{T}^{GRm}$ | $2.25\times10^{-4}$ | mM | Mitochondrial matrix concentration of GR | S34 | Adjusted |
| $E_{T}^{GRi}$ | $2.25\times10^{-4}$ | mM | Extra-matrix concentration of GR | S35 | Adjusted |
| $K_{M}^{NADPH}$ | 0.015 | mM | Michaelis constant for NADPH of GR | S34,S35 | (2) |
| $K_{M}^{GSSG}$ | 0.06 | mM | Michaelis constant for GSSG of GR | S34,S35 | (2) |
| $[NADPH]_i$ | $7.5\times10^{-2}$ | mM | Extra-matrix NADPH concentration | S34,S35 | (2) |
| $G_T$ | 6 | mM | Total pool of glutathione | S40,S41 | (2) |
| $k_{grx_m}$ | $3.6\times10^{-4}$ | mM $s^{-1}$ | Rate constant of mitochondrial matrix glutaredoxin reaction | S36 | (2) |
| $k_{grx_i}$ | $3.6\times10^{-4}$ | mM $s^{-1}$ | Rate constant of extra-matrix glutaredoxin reaction | S37 | (2) |

| | | | | | |
|---|---|---|---|---|---|
| $K_{eq}^{GRX}$ | 1.37×10$^{-3}$ | mM$^{-1}$ | Equilibrium constant of glutaredoxin | S36,S37 | (2) |
| $K_m^{Grx}$ | 0.01 | mM | Michaelis constant for GSH of GRX | S36,S37 | (2) |
| $K_m^{PSSG}$ | 0.0005 | mM | Michaelis constant for glutathionylated protein of glutaredoxin | S36,S37 | (2) |
| $k_{PSH}^1$ | 0.64 | ms$^{-1}$ | Rate constant of protein glutathionylation | S38,S39 | (2) |
| $E_T^{PSH}$ | 8×10$^{-4}$ | mM | Concentration of proteins that can become glutathionylated | S38,S39 | (2) |
| $K_M^{GSH}$ | 0.75 | mM | Michaelis constant of GSH for glutathionylation | S38,S39 | (2) |
| $K_{act}^{H2O2}$ | 1×10$^{-3}$ | mM | Activation constant of $H_2O_2$ for protein glutathionylation | S38,S39 | (2) |
| $GrxT$ | 0.002 | mM | Glutaredoxin concentration | S38,S39 | (2) |
| $c_{GST}$ | 1.5×10$^{-8}$ | ms$^{-1}$ | Rate constant of glutathione transporter | S42 | (2) |
| $k_{0.5}^{GST}$ | 2.6 | mM | transport association constant of GSH | S42 | (2) |
| $E_T^{Prx3m}$ | 3.0×10$^{-3}$ | mM | Mitochondrial matrix concentration of Trx peroxidase (Prx) | S43 | (2) |
| $E_T^{Prx3i}$ | 0.1 | mM | Extra-matrix concentration Prx | S44 | (2) |
| $\Phi_{1Prx}$ | 3.83 | mM ms | Constant for TxPX activity | S43,S44 | (2) |
| $\Phi_{2Prx}$ | 1.85 | mM ms | Constant for TxPX activity | S43,S44 | (2) |
| $E_T^{TrxR2m}$ | 1.225×10$^{-4}$ | mM | Mitochondrial matrix concentration of TrxR2 | S45 | Adjusted |
| $E_T^{TrxRi}$ | 1.225×10$^{-4}$ | mM | Extra-matrix concentration of TrxR | S46 | Adjusted |
| $K_M^{TrxSS}$ | 0.035 | mM | Michaelis constant for oxidized Trx [Trx[SS]] of TrxR | S45,S46 | (2) |
| $K_{M,\,Trx}^{NADPH}$ | 0.012 | mM | Michaelis constant for NADPH of TrxR | S45,S46 | (2) |
| $k_{TrxR}^1$ | 22.75×10$^{-3}$ | ms$^{-1}$ | Rate constant of TrxR | S45,S46 | (2) |
| $TrxT_m$ | 0.025 | mM | Total pool of mitochondrial matrix thioredoxin | S47 | (2) |
| $TrxT_i$ | 0.05 | mM | Total pool of extra-matrix thioredoxin | S48 | (2) |

| | | | | | |
|---|---|---|---|---|---|
| $k_{CAT}^{1}$ | 17 | $mM^{-1}ms^{-1}$ | Rate constant of catalase (CAT) | S49 | (2) |
| $E_{CAT}^{T}$ | $1.0\times10^{-6}$ | mM | Extra-matrix concentration of CAT | S49 | (2) |
| $fr$ | $5.0\times10^{-2}$ | $mM^{-1}$ | Hydrogen peroxide inhibition factor of CAT | S49 | (2) |

Adjustments were made to several of the scavenging parameters for the cellular model to better approximate the experimental results for isolated myocytes undergoing high frequency pacing. Parameters not included in **Table S3** remain the same as those specified in **Table S2**.

**Table S3 Parameter values used in the simulations: ROS production and scavenging – cellular model**

| Symbol | Value | Units | Description | Eq | Reference |
|---|---|---|---|---|---|
| $\Phi_1$ | $5.0\times10^{-5}$ | mM ms | Constant for GPX activity | S32,S33 | Adjusted |
| $\Phi_2$ | 27 | mM ms | Constant for GPX activity | S32,S33 | Adjusted |
| $E_T^{GPXm}$ | $9.77\times10^{-5}$ | mM | Mitochondrial matrix concentration of GPX | S32 | Adjusted |
| $\mathrm{E_T^{GRm}}$ | $2.3\times10^{-3}$ | mM | Mitochondrial matrix concentration of GR | S34 | Adjusted |
| $\mathrm{K_M^{NADPH}}$ | $6.54\times10^{-2}$ | mM | Michaelis constant for NADPH of mitochondrial GR | S34,S35 | Adjusted |
| $\mathrm{K_M^{GSSG}}$ | $20.6\times10^{-3}$ | mM | Michaelis constant for GSSG of mitochondrial GR | S34,S35 | (10) |
| $\mathrm{G_{T,mito}}$ | 1 | mM | Total mitochondrial pool of glutathione | S40,S41 | Adjusted |
| $\mathrm{G_{T,cyto}}$ | 2 | mM | Total cytosolic pool of glutathione | S40,S41 | (11) |
| $E_T^{PSH}$ | 0 | mM | Concentration of proteins that can become glutathionylated | S38,S39 | |
| $GrxT$ | 0 | mM | Glutaredoxin concentration | S38,S39 | |
| $c_{GST}$ | 0 | $ms^{-1}$ | Rate constant of glutathione transporter | S42 | |
| $\mathrm{E_T^{TrxR2m}}$ | $3.5\times10^{-4}$ | mM | Mitochondrial matrix concentration of TrxR2 | S45 | (2) |
| $\mathrm{E_T^{TrxRi}}$ | $3.5\times10^{-4}$ | mM | Extra-matrix concentration of TrxR | S46 | (2) |
| $\mathrm{K_{M,\,Trx}^{NADPH}}$ | 0.065 | mM | Michaelis constant for NADPH of TrxR | S45,S46 | Adjusted |

## Mitochondrial NADPH handling – mitochondrial model

In this section we will provide a detailed description of the mitochondrial NADPH handling.

$$NADPm = C_{NADPm} - [NADPH]_m \quad \text{(S50)}$$

$$V_{IDP\_NADP} = \left(1 + \frac{[H^+]_m}{k^{H+}_{m\_IDP}}\right)\left(1 + \frac{[ISOC]}{k^{ISOC}_{m\_IDP}} + \frac{NADP_m}{k^{NADP}_{m\_IDP}}\left(1 + \frac{k^{NADP}_{i\_IDP}}{NADP_m}\right) + \frac{[aKG]}{k^{aKG}_{m\_IDP}} + \frac{[NADPH_m]}{k^{NADPH}_{m\_IDP}} + \frac{[ISOC]}{k^{ISOC}_{m\_IDP}}\frac{NADP_m}{k^{NADP}_{m\_IDP}}\left(1 + \frac{k^{NADP}_{i\_IDP}}{NADP_m}\right) + \frac{[aKG]}{k^{aKG}_{m\_IDP}}\frac{[NADPH_m]}{k^{NADPH}_{m\_IDP}} + \frac{[ISOC]}{k^{ISOC}_{m\_IDP}}\frac{[NADPH_m]}{k^{NADPH}_{m\_IDP}} + \frac{[aKG]}{k^{aKG}_{m\_IDP}}\frac{NADP_m}{k^{NADP}_{m\_IDP}}\left(1 + \frac{k^{NADP}_{i\_IDP}}{NADP_m}\right)\right)$$ (S51)

$$V_{IDH_{NADP}} = \frac{V_f^{IDH}\frac{k[ISOC]NADP_m}{k^{ISOC}_{m\_IDP}k^{NADP}_{m\_IDP}}\left(1+\frac{k^{NADP}_{i\_IDP}}{VNADH_m}\right) - V_b^{IDH}\frac{[aKG]\ [NADP_m]}{k^{aKG}_{m\_IDP}k^{NADPH}_{m\_IDP}}}{V_{IDP\_NADP}}$$ (S52)

$$V_{THDen} = 1 + \frac{[NADH_m]}{k^{NADHm}_{m\_THD}} + \frac{NAD}{k^{NAD}_{m\_THD}} + \frac{NADP_m}{k^{NADP}_{m\_THD}} + \frac{[NADPH_m]}{k^{NADPH}_{m\_THD}} + \frac{[NADH_m]}{k^{NADHm}_{m\_THD}}\frac{NADP_m}{k^{NADP}_{m\_THD}}e^{(F/10RT).\Delta\mu_H} + \frac{[NADPH_m]}{k^{NADPH}_{m\_THD}}\frac{[NADH_m]}{k^{NADHm}_{m\_THD}}e^{(1-(F/10RT).\Delta\mu_H)} + \frac{NAD}{k^{NAD}_{m\_THD}}\frac{NADP_m}{k^{NADP}_{m\_THD}}e^{(F/10RT)\Delta\mu_H}.e^{(1-(F/10RT).\Delta\mu_H)} + \frac{[NADH_m]}{k^{NADHm}_{m\_THD}}\frac{[NADPH_m]}{k^{NADPH}_{m\_THD}}$$ (S53)

$$V_{THD} = \frac{E_T^{THD}.k_a^{THD}\frac{[NADH]_m NADP_m}{k^{NADHm}_{m\_THD}\ k^{NADP}_{m\_THD}}e^{(F/10RT).\Delta\mu_H} - E_T^{THD}.k_b^{THD}\frac{NAD\ \ [NADPH_m]}{k^{NAD}_{m\_THD}\ k^{NADPH}_{m\_THD}}e^{(1-(F/10RT).\Delta\mu_H)}}{V_{THDen}}$$ (S54)

**Table S4 Parameter values used in the simulations: Mitochondrial NADPH handling – mitochondrial model**

| Symbol | Value | Units | Description | Eq. | Reference |
|---|---|---|---|---|---|
| $C_{NADPm}$ | 0.1 | mM | Sum of NADPH plus $NADP^+$ | S50 | (2) |
| $k^{H+}_{m\_IDP}$ | 0.5 | mM | Dissociation constant for $H^+$ of IDH2 | S51 | (2) |
| $k^{ISOC}_{m\_IDP}$ | $3.9\times10^{-3}$ | mM | Michaelis constant for ISOC in IDH2 | S51,S52 | (2) |
| $k^{NADP}_{m\_IDP}$ | $6.7\times10^{-3}$ | mM | Michaelis constant for NADP in IDH2 | S51,S52 | (2) |
| $k^{NADP}_{i\_IDP}$ | $2\times10^{-6}$ | mM | Inhibition constant for NADP in IDH2 | S51,S52 | (2) |
| $k^{NADPH}_{m\_IDP}$ | $1.2\times10^{-2}$ | mM | Michaelis constant for NADPH in IDH2 | S51,S52 | (2) |
| $k^{aKG}_{m\_IDP}$ | 0.51 | mM | Michaelis constant for αKG in IDH2 | S51,S52 | (2) |
| $V_f^{IDH}$ | 8.72×10-5 | mM $ms^{-1}$ | Maximal rate of IDH2 in the forward direction | S52 | (2) |
| $V_b^{IDH}$ | $5.45\times10^{-6}$ | mM $ms^{-1}$ | Maximal rate of IDH2 in the reverse direction | S52 | (2) |
| $k^{NADPH}_{m\_THD}$ | 0.02 | mM | Michaelis constant for NADPH in transhydrogenase (THD) | S53,S54 | (2) |
| $k^{NADHm}_{m\_THD}$ | 0.01 | mM | Michaelis constantfor NADH in THD | S53,S54 | (2) |
| $k^{NAD}_{m\_THD}$ | 0.125 | mM | Michaelis constant for NAD in THD | S53,S54 | (2) |
| $k^{NADP}_{m\_THD}$ | 0.017 | mM | Michaelis constant for NADP in THD | S53,S54 | (2) |

| | | | | | |
|---|---|---|---|---|---|
| $E_T^{THD}$ | 1.1875×10$^{-5}$ | mM | Concentration of THD enzyme | S54 | (2) |
| $k_f^{THD}$ | 1.17474 | ms$^{-1}$ | Forward catalytic constant of THD | S54 | (2) |
| $k_b^{THD}$ | 10 | ms$^{-1}$ | Reverse catalytic constant of THD | S54 | (2) |

## Mitochondrial NADPH handling – cellular model

In this section we will provide a detailed description of the mitochondrial NADPH handling.

$$V_{THD} = \frac{E_T^{THD}.k_a^{THD}\frac{[NADH]_m NADPm}{k_{m\_THD}^{NADHm}\ k_{m\_THD}^{NADP}}e^{(xdF/RT).\Delta\mu_H} - E_T^{THD}.k_b^{THD}\frac{NAD\ \ [NADPH_m]}{k_{m\_THD}^{NAD}\ k_{m\_THD}^{NADPH}}e^{(x(d-1)F/RT).\Delta\mu_H)}}{V_{THDen}} \quad \text{(S54)}$$

**Table S5 Parameter values used in the simulations: Mitochondrial NADPH handling – cellular model**

| Symbol | Value | Units | Description | Eq. | Reference |
|---|---|---|---|---|---|
| $k_{m\_IDP}^{ISOC}$ | 0.045 | mM | Michaelis constant for ISOC in IDH2 | S51,S52 | (12) |
| $k_{m\_IDP}^{NADP}$ | 0.046 | mM | Michaelis constant for NADP in IDH2 | S51,S52 | (12) |
| $k_{i\_IDP}^{NADP}$ | 2×10$^{-6}$ | mM | Inhibition constant for NADP in IDH2 | S51,S52 | (2) |
| $k_{m\_IDP}^{NADPH}$ | 1.2×10$^{-2}$ | mM | Michaelis constant for NADPH in IDH2 | S51,S52 | (2) |
| $k_{m\_IDP}^{aKG}$ | 0.080 | mM | Michaelis constant for αKG in IDH2 | S51,S52 | (12) |
| $V_f^{IDH}$ | 8.72×10$^{-2}$ | mM ms$^{-1}$ | Maximal rate of IDH2 in the forward direction | S52 | Adjusted |
| $V_{fb}^{IDH}$ | 5.45×10$^{-3}$ | mM ms$^{-1}$ | Maximal rate of IDH2 in the reverse direction | S52 | Adjusted |
| $k_{m\_THD}^{NADPH}$ | 4×10$^{-3}$ | mM | Michaelis constant for NADPH in transhydrogenase (THD) | S53,S54 | Adjusted |
| $k_{m\_THD}^{NADHm}$ | 0.01 | mM | Michaelis constant for NADH in THD | S53,S54 | (2) |
| $k_{m\_THD}^{NAD}$ | 0.125 | mM | Michaelis constant for NAD in THD | S53,S54 | (2) |
| $k_{m\_THD}^{NADP}$ | 0.02 | mM | Michaelis constant for NADP in THD | S53,S54 | Adjusted |
| $E_T^{THD}$ | 1×10$^{-3}$ | mM | Concentration of THD enzyme | S54 | Adjusted |
| $k_f^{THD}$ | 1.17474 | ms$^{-1}$ | Forward catalytic constant of THD | S54 | (2) |
| $k_b^{THD}$ | 17.2756 | ms$^{-1}$ | Reverse catalytic constant of THD | S54 | Adjusted |

| | | |
|---|---|---|
| d | 0.5 | (13) |
| x | 0.1 | (13) |

## Mitochondrial Model of Energy Metabolism and ion dynamics

The detailed explanation of the mathematical expressions and parameters of the model were previously presented in Wei et al. (2011).

### Computational modeling of $Na^+/H^+$ exchanger (NHE) and phosphate carrier (PiC)

$$J_{NHE} = c_{NHE} \frac{\beta_1^+ \beta_2^+ - \beta_1^- \beta_2^-}{\beta_1^+ + \beta_1^- + \beta_2^+ + \beta_2^-} \Big/ \left(1 + 10^{n_i (pH_i - pK_i)}\right)$$

where

$$\beta_1^+ = \frac{k_1^+ K_{H\_NHE} [Na^+]_m}{K_{H\_NHE}[Na^+]_m + K_{H\_NHE} K_{Na\_NHE} + K_{Na\_NHE}[H^+]_m}$$

$$\beta_2^+ = \frac{k_4^+ K_{Na\_NHE} [H^+]_i}{K_{H\_NHE}[Na^+]_i + K_{H\_NHE} K_{Na\_NHE} + K_{Na\_NHE}[H^+]_i}$$

$$\beta_1^- = \frac{k_1^- K_{H\_NHE} [Na^+]_i}{K_{H\_NHE}[Na^+]_i + K_{H\_NHE} K_{Na\_NHE} + K_{Na\_NHE}[H^+]_i}$$

$$\beta_2^- = \frac{k_4^- K_{Na\_NHE} [H^+]_m}{K_{H\_NHE}[Na^+]_m + K_{H\_NHE} K_{Na\_NHE} + K_{Na\_NHE}[H^+]_m}$$

$$J_{PIC} = c_{PiC} \frac{V_{PIC,f} \frac{[H_2PO_4^{2-}]_i [OH^-]_m}{K_{Pi,i} K_{OH,m}} - V_{PIC,b} \frac{[H_2PO_4^{2-}]_m [OH^-]_i}{K_{Pi,m} K_{OH,i}}}{\left(1 + \frac{[H_2PO_4^{2-}]_i}{K_{Pi,i}} + \frac{[OH^-]_m}{K_{OH,m}} + \frac{[H_2PO_4^{2-}]_m}{K_{Pi,m}} + \frac{[OH^-]_i}{K_{OH,i}} + \frac{[H_2PO_4^{2-}]_m [OH^-]_i}{K_{Pi,m} K_{OH,i}} + \frac{[H_2PO_4^{2-}]_i [OH^-]_m}{K_{Pi,i} K_{OH,m}}\right)}$$

**Table S6 Parameter values for the mitochondrial Na+/H+ proton exchanger and phosphate carrier – mitochondrial and cellular models**

| Symbol | Value | Units | Description | Reference |
|---|---|---|---|---|
| $k_1^+$ | 0.0252 | $ms^{-1}$ | NHE forward rate constant | (2) |
| $k_1^-$ | 0.0429 | $ms^{-1}$ | NHE backward rate constant | (2) |
| $k_4^+$ | 0.16 | $ms^{-1}$ | NHE forward rate constant | (2) |
| $k_4^-$ | 0.0939 | $ms^{-1}$ | NHE backward rate constant | (2) |
| $K_{Na\_NHE}$ | 24 | mM | Na+Dissociation constant | (2) |
| $K_{H\_NHE}$ | $1.585\times10^{-4}$ | mM | H+Dissociation constant | (2) |
| $pK_i$ | 8.52 | | Proton inhibitory constant | (2) |
| $n_i$_NHE | 3 | | Hill coefficient for H+ binding | (2) |
| $c_{NHE}$ | 0.00785 (mitochondria) | mM | NHE concentration | (2) |
| $K_{Pi,i}$ | 11.06 | mM | Extra-matrix Pi binding constant | (2) |
| $K_{Pi,m}$ | 11.06 | mM | Mitochondrial matrix Pi binding constant | (2) |
| $K_{OH,i}$ | $4.08\times10^{-5}$ | mM | Extra-matrix OH- binding constant | (2) |
| $K_{OH,m}$ | $4.08\times10^{-5}$ | mM | Mitochondrial matrix OH- binding constant | (2) |
| $V_{PIC,f}$ | 90 | µmol $min^{-1}$ mg $protein^{-1}$ | Forward $V_{max}$ | (2) |
| $V_{PIC,b}$ | 90 | µmol $min^{-1}$ mg $protein^{-1}$ | Backward $V_{max}$ | (2) |
| $c_{PiC}$ | 4.9 | mg protein $ml^{-1}$ | PiC concentration | Adjusted |

## TCA cycle rate equations

$$V_{CS} = \frac{k_{cat}^{CS} E_T^{CS}}{\left(1+\frac{K_M^{AcCoA}}{[AcCoA]}\right)\left(1+\frac{K_M^{OAA}}{[OAA]}\right)}$$

$$V_{ACO} = k_f^{ACO}\left([CIT] - \frac{[ISOC]}{K_E^{ACO}}\right)$$

$$V_{IDH} = k_{cat}^{IDH} E_T^{IDH}\left[\begin{array}{l}\left(1+\frac{[H^+]_m}{k_{h,1}}+\frac{k_{h,2}}{[H^+]_m}\right)+ f_i^{IDH}\left(\frac{K_{Midh}^{NAD}}{[NAD]}\right)+\ldots \\ f_a^{IDH}\left(\frac{K_M^{ISOC}}{[ISOC]}\right)^{ni} + f_a^{IDH} f_i^{IDH}\left(\frac{K_M^{ISOC}}{[ISOC]}\right)^{ni}\left(\frac{K_{Midh}^{NAD}}{[NAD]}\right)\end{array}\right]^{-1}$$

$$f_a^{IDH} = \left[\left(1+\frac{[ADP^{3-}]_m}{K_{ADP}^a}\right)\left(1+\frac{[Ca^{2+}]_m}{K_{Ca}^a}\right)\right]^{-1}$$

$$f_i^{IDH} = \left(1+\frac{[NADH]}{K_{i,NADH}}\right)$$

$$V_{KGDH} = \frac{k_{cat}^{KGDH} E_T^{KGDH}}{1+\frac{[H^+]_m}{k_{h,1a}}+\frac{k_{h,2a}}{[H^+]_m}+ f_a^{KGDH}\left(\frac{k_M^{\alpha KG}}{[\alpha KG]}\right)^{n_{\alpha KG}} + f_a^{KGDH}\frac{k_{M\_kgdh}^{NAD}}{[NAD]}}$$

$$f_a^{KGDH} = \left[\left(1+\frac{[Mg^{2+}]}{K_D^{Mg^{2+}}}\right)\left(1+\frac{[Ca^{2+}]_m}{K_D^{Ca^{2+}}}\right)\right]^{-1}$$

$$V_{SL} = k_f^{SL}\left([SCoA][ADP]_m[Pi]_m - \frac{[Suc][ATP]_m[CoA]}{K_{E,app}^{SL}}\right)$$

$$K_{E,app}^{SL} = K_{Eq}^{SL}\frac{P_{SUC}P_{ATP}}{P_{Pi}P_{ADP}}$$

Succinate dehydrogenase is included in the Table comprising the respiratory complexes

$$V_{FH} = k_f^{FH}\left([FUM] - \frac{[MAL]}{K_E^{FH}}\right)$$

$$V_{MDH} = \frac{k_{cat}^{MDH} E_T^{MDH} f_{h,a} f_{h,i}}{1+\frac{K_M^{MAL}}{[MAL]}\left(1+\frac{[OAA]}{K_i^{OAA}}\right)+\frac{K_M^{NAD}}{[NAD]}+\frac{K_M^{MAL}}{[MAL]}\left(1+\frac{[OAA]}{K_i^{OAA}}\right)\frac{K_M^{NAD}}{[NAD]}}$$

$$f_{h,a} = \left(1 + \frac{[H^+]}{k_{h1}} + \frac{[H^+]^2}{k_{h1}k_{h2}}\right)^{-1} + k_{offset}$$

$$f_{h,i} = \left(1 + \frac{k_{h3}}{[H^+]} + \frac{k_{h3}k_{h4}}{[H^+]^2}\right)$$

$$V_{AAT} = k_f^{AAT}[OAA][GLU]\frac{k_{ASP}K_E^{ATT}}{\left(k_{ASP}K_E^{AAT} + [\alpha KG]k_f^{AAT}\right)}$$

**Table 7 Parameter values used in the simulations: Tricarboxylic acid cycle -- mitochondrial model**

| Symbol | Value | Units | Description | Reference |
|---|---|---|---|---|
| [AcCoA] | $1\times10^{-5}$-1 | mM | Acetyl CoA concentration | (2) |
| $k_{cat}^{CS}$ | $2.3523\times10^{-4}$ | $ms^{-1}$ | Catalytic constant of CS | (2)* |
| $E_T^{CS}$ | 0.4 | mM | Concentration of CS | (2) |
| $K_M^{AcCoA}$ | 0.0126 | mM | Michaelis constant for AcCoA | (2) |
| $K_M^{OAA}$ | $6.4\times10^{-4}$ | mM | Michaelis constant for OAA | (2) |
| $C_{k\,\mathrm{int}}$ | 1.3 | mM | Sum of TCA cycle intermediates | (2) |
| $k_f^{ACO}$ | $1.1688\times10^{-4}$ | $ms^{-1}$ | Forward rate constant of ACO | (2)* |
| $K_E^{ACO}$ | 2.22 | | Equilibrium constant of ACO | (2) |
| $K_{i,NADH}$ | 0.19 | mM | Inhibition constant by NADH | (2) |
| $k_{cat}^{IDH}$ | 11.88 | $ms^{-1}$ | Rate constant of IDH | (2)* |
| $E_T^{IDH}$ | 0.109 | mM | Concentration of IDH | (2) |
| $k_{h,1}$ | $1\times10^{-5}$ | mM | Inoization constant of IDH | (2) |
| $k_{h,2}$ | $9\times10^{-4}$ | mM | Inoization constant of IDH | (2) |
| $K_M^{ISOC}$ | 1.52 | mM | Michaelis constant for isocitrate | (2) |
| $n_i$ | 2.0 | | Cooperativity for isocitrate | (2) |

| | | | | |
|---|---|---|---|---|
| $K_{Midh}^{NAD}$ | 0.923 | mM | Michaelis constant for $NAD^+$ | (2) |
| $K_{ADP}^{a}$ | 0.62 | mM | Activation constant by ADP | (2) |
| $K_{Ca}^{a}$ | $5\times10^{-4}$ | mM | IDH activation constant for $Ca^{2+}$ | (2) |
| $E_T^{KGDH}$ | 0.5 | mM | Concentration of KGDH | (2) |
| $k_{cat}^{KDGH}$ | 0.0132 | $ms^{-1}$ | Rate constant of KGDH | (2)* |
| $k_M^{\alpha KG}$ | 30 | mM | Michaelis constant for $\alpha$KG | (2) |
| $K_{M\_kgdh}^{NAD}$ | 38.7 | mM | Michaelis constant for $NAD^+$ of KGDH | (2) |
| $k_{h,1a}$ | $4\times10^{-5}$ | mM | Ionization constant of KGDH | (2) |
| $k_{h,2a}$ | $7\times10^{-5}$ | mM | Ionization constant of KGDH | (2) |
| $K_D^{Mg^{2+}}$ | 0.0308 | mM | Activation constant for $Mg^{2+}$ | (2) |
| $K_D^{Ca^{2+}}$ | $1.5\times10^{-4}$ | mM | Activation constant for $Ca^{2+}$ | (2) |
| $n_{\alpha KG}$ | 1.2 | | Hill coefficient of KGDH for $\alpha$ KG | (2) |
| $[Mg^{2+}]_m$ | 0.4 | mM | $Mg^{2+}$ concentration in mitochondria | (2) |
| $[Mg^{2+}]_i$ | 1.0 | mM | $Mg^{2+}$ concentration in cytosol/buffer | (2) |
| $k_f^{SL}$ | 0.028 | $mM^{-1}ms^{-1}$ | Forward rate constant of SL | (2)* |
| $K_E^{SL}$ | 3.115 | | Equilibrium constant of the SL reaction | (2) |
| [CoA] | 0.02 | mM | Coenzyme A concentrations. | (2) |
| $k_f^{FH}$ | $8.3\times10^{-3}$ | $ms^{-1}$ | Forward rate constant for FH. | (2)* |
| $K_E^{FH}$ | 1.0 | | Equilibrium constant of FH | (2) |
| $k_{h1}$ | $1.131\times10^{-5}$ | mM | Ionization constant of MDH | (2) |

| | | | | |
|---|---|---|---|---|
| $k_{h2}$ | 26.7 | mM | Ionization constant of MDH | (2) |
| $k_{h3}$ | $6.68\times10^{-9}$ | mM | Ionization constant of MDH | (2) |
| $k_{h4}$ | $5.62\times10^{-6}$ | mM | Ionization constant of MDH | (2) |
| $k_{offset}$ | $3.99\times10^{-2}$ | | Offset of MDH pH activation factor | (2) |
| $k_{cat}^{MDH}$ | 0.1242 | $ms^{-1}$ | Rate constant of MDH | (2)* |
| $E_T^{MDH}$ | 0.154 | mM | Total MDH enzyme concentration | (2) |
| $K_M^{MAL}$ | 1.493 | mM | Michaelis constant for malate | (2) |
| $K_i^{OAA}$ | 0.031 | mM | Inhibition constant for oxaloacetate | (2) |
| $K_M^{NAD}$ | 0.2244 | mM | Michaelis constant for $NAD^+$ | (2) |
| [GLU] | $1\times10^{-5}$ - 30 | mM | Glutamate concentration. | (2) |
| $k_f^{AAT}$ | 0.0214 | $ms^{-1}$ | Forward rate constant of AAT | (2)* |
| $K_E^{AAT}$ | 6.6 | | Equilibrium constant of AAT | (2) |
| $k_{ASP}$ | $1.5\times10^{-6}$ | $ms^{-1}$ | Rate constant of aspartate consumption | (2) |

*While these parameters may differ from the supplement of Kembro et al., they were taken from code provided by those authors that successfully reproduces the figures from the paper.

**Table 8 Parameter values used in the simulations: Tricarboxylic acid cycle -- mitochondrial model**

| Symbol | Value | Units | Description | Reference |
|---|---|---|---|---|
| [AcCoA] | 1 | mM | Acetyl CoA concentration | (2) |
| $k_{cat}^{CS}$ | $1.5891\times10^{-4}$ | $ms^{-1}$ | Catalytic constant of CS | (2)* |
| $k_f^{ACO}$ | $7.8959\times10^{-5}$ | $ms^{-1}$ | Forward rate constant of ACO | (2)* |
| $k_{cat}^{IDH}$ | 0.5350 | $ms^{-1}$ | Rate constant of IDH | (2)* |

| | | | | |
|---|---|---|---|---|
| $k_{cat}^{KDGH}$ | 0.0179 | $ms^{-1}$ | Rate constant of KGDH | (2)* |
| $k_f^{SL}$ | 0.0284 | $mM^{-1}ms^{-1}$ | Forward rate constant of SL | (2)* |
| $k_f^{FH}$ | $8.4\times10^{-3}$ | $ms^{-1}$ | Forward rate constant for FH. | (2)* |
| $k_{cat}^{MDH}$ | 0.1259 | $ms^{-1}$ | Rate constant of MDH | (2)* |
| [GLU] | 30 | mM | Glutamate concentration. | (2) |
| $k_f^{AAT}$ | 0.0217 | $ms^{-1}$ | Forward rate constant of AAT | (2)* |

Oxidative phosphorylation equations for the mitochondrial model are the same as for Gauthier et al. (14) with the exception of $k_{010}$, which was increased from 50 to 600 to match experimental data from Aon et al. 2012 (1) on ROS production from isolated mitochondria. Rate constants were scaled to yield fluxes in /ms units. Parameter changes for the cellular model are noted below.

**Table 9 Parameter values used in the simulations: electron transport chain -- cellular model**

| Symbol | Value | Units | Description | Reference |
|---|---|---|---|---|
| $\rho_{c1}$ | 24.9302 | mM | Complex I concentration | Adjusted |
| $a_{61}$* | $3.3290\times10^{7}$ | mM/s | | Adjusted |
| $a_{16}$* | 432.7642 | mM/s | | Adjusted |
| $k_{010}$ | 1700 | mM/min | Reverse reaction constant for reduction of oxygen by $SQ_p$ | Adjusted |

**Table 10 Parameter values used in the simulations: oxidative phosphorylation -- mitochondrial model**

| Symbol | Value | Units | Description | Reference |
|---|---|---|---|---|
| $p_1$ | $1.346\times10^{-4}$ | | Sum of products of rate constants | |
| $p_2$ | $7.739\times10^{-7}$ | | Sum of products of rate constants | |
| $p_3$ | $6.65\times10^{-15}$ | | Sum of products of rate constants | |
| $\rho^{F1}$ | 5 | mM | Concentration of $F_1F_0$-ATPase | (2) |

| | | | | |
|---|---|---|---|---|
| $K_{eq}^{ATPase}$ | $1.71\times10^{6}$ | | Equilibrium constant of ATP synthesis | |
| $[Pi]_i$ | 3 | mM | Inorganic phosphate concentration | |
| $C_A$ | 1.01 | mM | Total sum of adenine nucleotides | (2)* |
| $V_{maxANT}$ | 3.15 | mM $ms^{-1}$ | Maximal rate of the ANT | (2) |
| $h^{ANT}$ | 0.5 | | Fraction of $\Delta\Psi_B$ | |
| $g_H$ | $2\times10^{-6}$ | mM $ms^{-1}$ $mV^{-1}$ | Ionic conductance of the inner membrane | (2) |
| $C_{PN}$ | 1.0 | mM | Total sum of pyridine nucleotides | |
| $C_{mito}$ | $1.812\times10^{-3}$ | mM $mV^{-1}$ | Inner membrane capacitance | |

**Table 11 Parameter values used in the simulations: oxidative phosphorylation -- cellular model**

| Symbol | Value | Units | Description | Reference |
|---|---|---|---|---|
| $\rho^{F1}$ | 5 | mM | Concentration of $F_1F_0$-ATPase | Adjusted |

**Table 12 Parameter values used in the simulations: Mitochondrial $Ca^{2+}$ handling – mitochondrial model**

| Symbol | Value | Units | Description |
|---|---|---|---|
| $V_{\max}^{uni}$ | $4.46\times10^{-3}$ | mM $ms^{-1}$ | $V_{max}$uniporter $Ca^{2+}$ transport |
| $\Delta\Psi^{\circ}$ | 91 | mV | Offset membrane potential |
| $K_{act}$ | $3.8\times10^{-4}$ | mM | Activation constant |
| $K_{trans}$ | 0.019 | mM | $K_d$ for translocated $Ca^{2+}$ |
| $L$ | 110.0 | | $K_{eq}$ for conformational transitions in uniporter |
| $n_a$ | 2.8 | | Uniporter activation cooperativity |
| $V_{\max}^{NaCa}$ | $1.83\times10^{-4}$ | mM $ms^{-1}$ | $V_{max}$ of $Na^+/Ca^{2+}$ exchanger |
| $b$ | 0.5 | | $\Delta\Psi_m$ dependence on $Na^+/Ca^{2+}$ exchanger |

| | | | |
|---|---|---|---|
| $K_{Na}$ | 9.4 | mM | Exchanger $Na^{2+}$ constant |
| $K_{Ca}$ | $3.75\times10^{-4}$ | mM | Exchanger $Ca^{2+}$ constant |
| $n$ | 3.0 | | $Na^{+}/Ca^{2+}$ exchanger cooperativity |
| $\delta_{Ca}$ | $3\times10^{-4}$ | | Fraction of free $[Ca^{2+}]_m$ |

**Table 13 Parameter values used in the simulations: Mitochondrial $Ca^{2+}$ handling – cellular model**

| Symbol | Value | Units | Description | Reference |
|---|---|---|---|---|
| $V_{\max}^{uni}$ | $1.2295\times10^{-4}$ | mM $ms^{-1}$ | $V_{max}$uniporter $Ca^{2+}$ transport | Adjusted |
| $V_{\max}^{NaCa}$ | $4.6650\times10^{-5}$ | mM $ms^{-1}$ | $V_{max}$ of $Na^{+}/Ca^{2+}$ exchanger | Adjusted |

For Ru360 protocols, Vuni was 99% blocked. For CGP protocols, VNaCa was 85% blocked.

**Table 14 Parameter values used in the simulations: Mitochondrial $H^{+}$ and $Na^{+}$ handling – mitochondrial model**

| Symbol | Value | Units | Description | Reference |
|---|---|---|---|---|
| $\delta_H$ | $1\times10^{-5}$ | dimensionless | mitochondria $H^{+}$ buffering capacity | (2) |
| $K_{a,ADP}$ | $4.17\times10^{-7}$ | | ADP dissociation constant | (2) |
| $K_{a,ATP}$ | $3.31\times10^{-7}$ | | ATP dissociation constant | (2) |
| $K_{a,Pi}$ | $1.78\times10^{-7}$ | | Pi dissociation constant | (2) |
| $K_{Mg,ATP}$ | $6.46\times10^{-5}$ | | $Mg^{2+}$ATP dissociation constant | (2) |
| $K_{Mg,ADP}$ | $5.62\times10^{-4}$ | | $Mg^{2+}$ADP dissociation constant | (2) |
| $K_{a,SUC}$ | $6.3\times10^{-6}$ | | Ka of succinate dissociation constant | (2) |
| $K_{a,H_2O}$ | $1\times10^{-14}$ | M | dissociation constant for water | (2) |
| $[H^{+}]_i$ | $1\times10^{-4}$ | mM | cytosolic $H^{+}$ concentration | (2) |
| $[Na^{+}]_i$ | 10 | mM | cytosolic $Na^{+}$ concentration | (2)* |
| $[Ca^{2+}]_i$ | $1\times10^{-4}$ | mM | cytosolic $Ca^{2+}$ concentration | (2) |
| $[ADP]_i$ | 0.01~1.0 | mM | cytosolic ADP concentration | (2) |

**Table 15 Parameter values used in the simulations: Mitochondrial $H^+$ and $Na^+$ handling – cellular model**

| Symbol | Value | Units | Description | Reference |
|---|---|---|---|---|
| $[Na^+]_i$ | 5-15 | mM | cytosolic $Na^+$ concentration | (15) |
| $[Ca^{2+}]_i$ | $1\times10^{-4}$ | mM | diastolic cytosolic $Ca^{2+}$ concentration | (2) |

Control Nai is 5mM, heart failure simulations used 15mM.

**Table 16 Parameter values used in the simulations: ROS transport – mitochondrial and cellular models**

| Symbol | Value | Units | Description | Reference |
|---|---|---|---|---|
| $a$ | $1\times10^{-3}$ | dimensionless | Basal IMAC conductance | (2) |
| $b$ | $1\times10^{4}$ | dimensionless | Activation factor by cytoplasmic $O_2^{\cdot-}$ | (2) |
| $K_{cc}$ | $1\times10^{-2}$ | mM | Activation constant by cytoplasmic $O_2^{\cdot-}$ | (2) |
| GL | $3.5\times10^{-8}$ | | Integral conductance for IMAC | (2) |
| $G_{max}$ | $3.9085\times10^{-6}$ | | Leak conductance of IMAC at saturation | (2) |
| K | $7.0\times10^{-2}$ | $mV^{-1}$ | Steepness factor | (2) |
| $\Delta\Psi_m^b$ | 4 | mV | Potential at half saturation | (2) |
| j | 0.1 | dimensionless | Fraction of IMAC conductance | (2) |
| $\frac{RT}{F}$ | 26.730818 | | | (2) |


1. Aon, M. A., B. A. Stanley, V. Sivakumaran, J. M. Kembro, B. O'Rourke, N. Paolocci, and S. Cortassa. 2012. Glutathione/thioredoxin systems modulate mitochondrial H2O2 emission: An experimental-computational study. The Journal of general physiology 139:479-491.
2. Kembro, J. M., M. A. Aon, R. L. Winslow, B. O'Rourke, and S. Cortassa. 2013. Integrating Mitochondrial Energetics, Redox and ROS Metabolic Networks: A Two-Compartment Model. Biophysical journal 104:332-343.

3. Cortassa, S., M. A. Aon, R. L. Winslow, and B. O'Rourke. 2004. A mitochondrial oscillator dependent on reactive oxygen species. Biophysical journal 87:2060-2073.
4. Fernandes, A. P., and A. Holmgren. 2004. Glutaredoxins: glutathione-dependent redox enzymes with functions far beyond a simple thioredoxin backup system. Antioxidants & redox signaling 6:63-74.
5. Holmgren, A. 1989. Thioredoxin and glutaredoxin systems. J Biol Chem 264:13963-13966.
6. Cox, A. G., C. C. Winterbourn, and M. B. Hampton. 2010. Mitochondrial peroxiredoxin involvement in antioxidant defence and redox signalling. Biochem J 425:313-325.
7. Sztajer, H., B. Gamain, K. D. Aumann, C. Slomianny, K. Becker, R. Brigelius-Flohe, and L. Flohe. 2001. The putative glutathione peroxidase gene of Plasmodium falciparum codes for a thioredoxin peroxidase. J Biol Chem 276:7397-7403.
8. Pillay, C. S., J. H. Hofmeyr, B. G. Olivier, J. L. Snoep, and J. M. Rohwer. 2009. Enzymes or redox couples? The kinetics of thioredoxin and glutaredoxin reactions in a systems biology context. Biochem J 417:269-275.
9. Eckenroth, B., K. Harris, A. A. Turanov, V. N. Gladyshev, R. T. Raines, and R. J. Hondal. 2006. Semisynthesis and characterization of mammalian thioredoxin reductase. Biochemistry 45:5158-5170.
10. Carlberg, I., and B. Mannervik. 1984. Glutathione reductase. Methods in enzymology 113:484-490.
11. Zhou, L., S. Cortassa, A.-C. Wei, M. A. Aon, R. L. Winslow, and B. O'Rourke. 2009. Modeling Cardiac Action Potential Shortening Driven by Oxidative Stress-Induced Mitochondrial Oscillations in Guinea Pig Cardiomyocytes. Biophysical journal 97:1843-1852.
12. Popova, T., M. A. Carvalho, L. Matasova, and L. Medvedeva. 2007. Regulation of mitochondrial NADP-isocitrate dehydrogenase in rat heart during ischemia. Molecular and Cellular Biochemistry 294:97-105.
13. Sazanov, L. A., and J. B. Jackson. 1994. Proton-translocating transhydrogenase and NAD- and NADP-linked isocitrate dehydrogenases operate in a substrate cycle which contributes to fine regulation of the tricarboxylic acid cycle activity in mitochondria. FEBS Letters 344:109-116.
14. Gauthier, L. D., J. L. Greenstein, S. Cortassa, B. O'Rourke, and R. L. Winslow. 2013. A Computational Model of Reactive Oxygen Species and Redox Balance in Cardiac Mitochondria. Biophysical Journal 105:1045-1056.
15. Kohlhaas, M., T. Liu, A. Knopp, T. Zeller, M. F. Ong, M. Böhm, B. O'Rourke, and C. Maack. 2010. Elevated cytosolic Na+ increases mitochondrial formation of reactive oxygen species in failing cardiac myocytes. Circulation 121:1606-1613.